Multivalent Carbocyanine Molecular Probes: Synthesis and Applications[§]

Yunpeng Ye,[†] Sharon Bloch,[†] Jeffery Kao,[‡] and Samuel Achilefu*,[†]

Department of Radiology and Department of Chemistry, Washington University, St. Louis, Missouri 63110.
Received August 31, 2004; Revised Manuscript Received October 18, 2004

Synergistic multivalent interactions can amplify desired chemical or biological molecular recognitions. We report a new class of multicarboxylate-containing carbocyanine dye constructs for use as optical scaffolds that not only serve as fluorescent antennas but also participate in structural assembly of the multivalent molecular construct. Three generations of carboxylate-terminating multivalent near-infrared carbocyanine probes from a dicarboxylic acid precursor dye (cypate) were prepared via its imino diacetic acid derivatives. Conjugation of the probes with D-(+)-glucosamine afforded dendritic arrays of the carbohydrates on an inner NIR chromophore core. All the multicarboxylate probes and their glucosamine conjugates have similar NIR spectral properties because conjugation occurred at distal positions to the inner chromophore core, thereby providing consistent and predictable spectral properties for their biological applications. Although light-induced photodamage equally affected the precursor dye, multicarboxylate probes, and their glucosamine derivatives, we observed that octacarboxylcypate (multivalent probe) was remarkably stable in different mediums at physiologically relevant temperatures relative to cypate, especially in basic mediums. Biodistribution studies in tumor-bearing nude mice show that all the glucosamine conjugates localized in the tumor but cypate was almost exclusively retained in the liver at 24 h postinjection. The tumor uptake does not correlate with the number of glucosamine tether on the multicarboxylate probe. Overall, the triglucosamine derivative appears to offer the best balance between high tumor uptake and low retention in nontarget tissues. These results suggest that multivalent molecular beacons are useful for assessing the beneficial effects of multivalency and for optimizing the biological and chemical properties of tissue-specific molecular probes.

INTRODUCTION

Optical imaging is attractive for studying molecular recognitions of chemical and biological importance because minute fluorescent tracers can be detected in homogeneous and heterogeneous media with existing laboratory instruments. For in vivo biological applications, near-infrared (NIR) fluorescent carbocyanine molecular probes are valuable for optical imaging because light in the 700−900 nm wavelengths propagates several centimeters in tissue (*1*, *2*). As a result, diseases in deep tissues can be monitored noninvasively by NIR optical methods. Additionally, NIR excitation also minimizes tissue autofluorescence that confounds spectral analysis in the visible wavelengths. Thus, development of NIR molecular probes with high specificity, selectivity, sensitivity, and stability are highly desirable.

Several reports have successfully demonstrated the potential of NIR dye bioconjugates for imaging diseases in small animals (*3*−*5*). Recent studies have focused on developing dye conjugates of small bioactive molecules to improve rapid diffusion to target tissue, identify, and optimize new molecular beacons by combinatorial library and high throughput strategies and enhance in vivo stability of the compounds (*4*, *6*−*10*). Most of these studies were performed with carbocyanine-based molecular probes because of the exceptionally high biocompatibility and desirable spectral properties of indocyanine green (ICG), which is a member of this class of compounds (*7*, *11*). Because ICG itself does not readily react with biomolecules, we recently developed a reactive carbocyanine dye called cypate (**1**), which has similar spectral, blood clearance, and excretion profiles as ICG (*12*). Bioconjugates of cypate are not toxic to animals up >10 μmol/kg body weight. Despite these successes, direct labeling of bioactive molecules to optimize the probes for clinical applications remains a challenge.

Synthetic dendrimers, nanoparticles, quantum dots, and other polyvalent compounds use synergistic multivalent interactions to amplify desired chemical or biological molecular recognitions (*13*−*15*). Labeling the multivalent materials at their reactive peripheral sites with fluorescent antennas provides a highly sensitive approach to track, visualize, and quantify different molecular interactions by optical methods. Although this strategy allows for conjugating multiple chromophores, the resulting molecular constructs may quench fluorescence, induce aggregation, disrupt bioactive conformations of adjacent small molecules, and destabilize the chromophore systems because of their exposure to harsh and metabolically active mediums.

Recently, we reported a new class of multicarboxylate-containing carbocyanine probes for use as optical scaffolds that not only serve as fluorescent antennas but also

* Corresponding author. Samuel Achilefu, Department of Radiology, Washington University School of Medicine, 4525 Scott Ave., CB 8225, St. Louis, MO 63110. Phone: 314-362-8599. Fax: 314-747-5191. E-mail: achilefus@mir.wustl.edu.

[†] Department of Radiology.

[‡] Department of Chemistry.

[§] Part of the Special Issue on Imaging Chemistry that began in issue 6, 2004. A preliminary description of this work was presented at the Symposium on Chemistry and Biological Applications of Imaging Agents and Molecular Beacons, at the spring 2004 National Meeting of the Americal Chemical Society.

10.1021/bc049790i CCC: $30.25
Published on Web 12/23/2004

participate in structural assembly of the multivalent molecular probes (*16*). The peripheral carboxylic acids that are distal to the chromophore core allow facile conjugation with biomolecules and retain the desirable NIR spectral properties of the dendritic molecule. Herein, we report the synthesis, spectral properties, stability, and biodistribution of multivalent NIR carbocyanine-based molecular probes. The results show that multivalent constructs have increased solution stability over the precursor dye in different mediums and physiologically relevant temperatures. Biodistribution of the glucosamine derivatives shows that the distribution of the compounds in target tumor does not correlate directly with the number of glucosamine moieties but reveals the potential of using multivalency to optimize molecular probes for different biomedical applications.

EXPERIMENTAL PROCEDURES

General. All solvents and chemicals were reagent grade and used without further purification. Benzotriazol-1-yloxy-tris(pyrrolidino)phosphonium hexafluorophosphate (PyBOP) and *N*-hydroxybenzotriazole (HOBt) were purchased from AnaSpec (San Jose, CA). Trifluoroacetic acid (TFA) and DIEA were purchased from Advanced ChemTech (Louisville, KY). Diisopropylcarbodiimide (DIC) and glutaconaldehyde dianilide monohydrochloride were purchased from Lancaster Synthesis (Windham, NH). Dichloromethane (DCM), *N*,*N*-dimethyformamide (DMF), methanol, and acetonitrile were from purchased from Fisher Scientific (Pittsburgh, PA). Other commercial chemicals were purchased from Aldrich (Milwaukee, WI). Mass spectra were obtained in dilute methanol solutions using Waters ZQ 4000 positive electrospray at cone voltage 67 V. All the compounds including the intermediates and final products were fully identified by ES-MS. The identity of final glucosamine conjugates were also confirmed by MALDI-TOF high-resolution mass spectrometry.

HPLC Purification and Analysis. HPLC analysis was performed on a Vydac C-18 column (250 × 4.6 mm) at a flow rate of 1.0 mL/min. Semipreparative HPLC was performed on a Vydac C-18 column (25 × 2.2 cm) at 9.5 mL/min. HPLC solvents consist of water containing 0.05% TFA (solvent A) and acetonitrile containing 0.05% TFA (solvent B). The elution protocol for analytical HPLC starts with 90% A for 1 min, followed by a linear gradient to 30% A over 20 min, held at 30% A for 5 min, continued to 10% A over 5 min, and finally returned to 90% A over 2 min. The elution profile was monitored by UV absorbance at 254 and 214 nm.

NMR Analysis. NMR spectra were recorded on a Varian Inova-600 (Varian Assoc., Palo Alto, CA) spectrometer, and the data were processed off-line with VNMR software. Proton and carbon chemical shifts were measured in ppm downfield from an external 3-(trimethylsilyl) propionic acid (TSP) standard. Proton spectra were obtained in DMSO-d_6 with a 5200-Hz spectral width collected into 32k data points using a 5.0 s preacquisition delay. Carbon spectra were obtained with a 27 000-Hz spectral width collected into 64k data points. The proton-detected heteronuclear multiple quantum coherence (HMQC) spectrum was recorded using a 0.5 s $^1H-^{13}C$ nulling period. The 90° ^1H pulse width was 9.5 μs, and the 90° ^{13}C pulse width was 14 μs. The proton spectral width was set to 5200 Hz and the carbon spectral width was set to 27 000 Hz. Phase sensitive 2D spectra were obtained by employing the Hypercomplex method. A 2 × 256 × 2048 data matrix with 64 scans per t1 value was collected. Gaussian line broadening was used in weighting both the t2 and the t1 dimensions. After 2D Fourier transform, the spectra resulted in 512 × 2048 data points, which were phase- and baseline-corrected in both dimensions.

UV−Vis and Emission Analysis. Absorbance spectra were measured on a Beckman Coulter DU 640 UV−visible spectrophotometer. Fluorescence spectra were recorded on a Fluorolog-3 fluorophotometer (JOBIN YVON/HORIBA, Edison, NJ). Stock solutions (1.0 mM) of the dye and its conjugates were prepared by dissolving each sample in anhydrous DMSO (99.99%). UV−vis and fluorescence measurements were carried out by sequentially adding 0.5−2.0 μL aliquots of the stock solutions via a micropipet into 3 mL of 20% aqueous DMSO solution or other solvents in a quartz cuvette. The mixtures were stirred briefly for equilibration prior to data acquisition.

1,1,2-Trimethyl[1H]-benz[*e*]indole-3-propanoic Acid. A mixture of 1,1,2-trimethyl-[1H]-benz[*e*]indole (40.0 g, 19.11 mmol) and 3-bromopropanoic acid (40.0 g, 26.15 mmol) in 1,2-dichlorobenzene (200 mL) was heated with stirring at 110 °C for 18 h. After the resulting mixture was cooled to room temperature, the precipitate was collected by filtration, followed by trituration in DCM to remove the unreacted material, and dried under vacuum to afford 1,1,2-trimethyl[1H]-benz[*e*]indole-3-propanoic acid (57 g, 82.4%). ESI-MS: 281.31 ($[MH]^+$).

Cypate (1). A solution of Ac_2O (1.20 g, 11.75 mmol) in DCM (5 mL) was added dropwise to a cooled, stirring suspension of glutaconaldehyde dianil monohydrochloride (2.84 g, 9.97 mmol) and DIEA (2.60 g, 20.11 mmol) in DCM (20 mL). The resulting clear solution was stirred for 1 h and added dropwise to a refluxing solution of 1,1,2-trimethyl[1H]-benz[*e*]indole-3-propanoic acid (8.2 g, 22.64 mmol) and sodium acetate (3.2 g, 39.01 mmol) in acetonitrile/water (95/5 mL). The mixture was refluxed for 16 h, cooled, filtered, and washed with acetonitrile, 5% HCl solution, and ethyl ether. About 6 g (85%) of **1** was obtained. ESI-MS: 625.34 ($[MH]^+$).

Tricarboxylic Acid-Containing Cypate Derivative (2). To a cooled solution of **1** (352.5 mg, 0.5 mmol) in DMF (15 mL) was added EDCI (114.6 mg, 0.6 mmol). After 20 min, HOBt (81.2 mg, 0.60 mmol) and di-*tert*-butyl iminodiacetate (147.0 mg, 0.60 mmol) were added. The mixture was stirred at room temperature for 2 h and concentrated. The residue was dissolved in DCM (35 mL), washed with HCl solution (1 M, 3 × 15 mL) and brine, and dried over $MgSO_4$. The filtrate was concentrated and purified by flash column chromatography using dichloromethane/methanol (100:6 v/v) to afford 154 mg (33%). ES-MS: 852.41 ($[MH]^+$).

The above compound (70 mg, 0.075 mmol) was dissolved in TFA (10 mL) and stirred for 1 h, concentrated, and dried to afford 59 mg of **2**, which was further purified by HPLC for both UV−vis and fluorescence assays. ES-MS: 740.28 ($[MH]^+$); HR-MS: 740.2987($[MH]^+$).

Tetracarboxylic Acid-Containing Cypate Derivative (3). The *tert*-butyl ester of **3** (348 mg, 60%) was prepared from **1** (352.5 mg, 0.5 mmol), EDCI (382.0 mg, 2.0 mmol), HOBt (270 mg, 2.0 mmol), and di-*tert*-butyl iminodiacetate (490.0 mg, 2.0 mmol), as described for **2** above. ES-MS: 1079.49 ($[MH]^+$).

The ester (200 mg, 0.17 mmol) was dissolved in TFA (30 mL) and stirred for 1 h, concentrated, and dried to afford 154 mg (97%) of **3**, which was further purified by HPLC for both UV−vis and fluorescence assays. ES-MS: 855.20 ($[MH]^+$).

Hexacarboxylic Acid-Containing Cypate Derivative (4). The *tert*-butyl ester of **4** (72.0 mg, 30%) was prepared from **2** (130 mg, 0.16 mmol), EDCI (275.1 mg, 1.44 mmol), HOBt (194.4 mg, 1.44 mmol), and a solution of di-*tert*-butyl iminodiacetate (352.8 mg, 1.44 mmol), as described for **2** above. ES-MS: 1422.60 ($[MH]^+$).

The ester (15 mg, 0.01 mmol) was dissolved in TFA (10 mL) and stirred for 1 h, concentrated, and dried to afford **4** (11 mg, 95%) which was further purified by HPLC for both UV−vis and fluorescence assays. ES-MS: 1085.23 ($[MH]^+$).

Octacarboxylic Acid-Containing Cypate Derivative (5). The *tert*-butyl ester of **5** (55.0 mg, 30%) was prepared from **3** (94 mg, 0.10 mmol), EDCI (229.2 mg, 1.20 mmol), HOBt (162 mg, 1.20 mmol), and a solution of di-*tert*-butyl iminodiacetate (196.0 mg, 0.80 mmol) in DMF (3 mL), as described for **2** above. (ES-MS: 1764.61 ($[MH]^+$).

The ester (25 mg, 0.0136 mmol) was dissolved in TFA (10 mL) and stirred for 2 h, concentrated, and dried to afford **5** (18 mg, 95%), which was further purified by HPLC for both UV−vis and fluorescence assays. ES-MS: 1315.21 ($[MH]^+$); HR-MS: 1315.5061($[MH]^+$).

Mono-D-(+)-glucosamine-Containing Cypate (6). To a cooled (−5 °C) solution of **1** (15 mg, 0.0213 mmol), HBTU (10.26 mg, 0.027 mmol), and HOBt (3.7 mg, 0.027 mmol) in DMF (5 mL) was added a solution of D-(+) glucosamine·HCl (12.0 mg, 0.054 mmol) and DIEA (14 mg, 0.108 mmol) in DMSO (1 mL). The mixture was stirred at room temperature for 2 h and added into ether (25 mL) with stirring. The precipitate was collected and purified by HPLC (10%-80% of A over 30 min) to afford 2.4 mg (13%) of **6**. ES-MS: 786.30 ($[MH]^+$); HR-MS: 786.4157 ($[MH]^+$).

Di-D-(+)-glucosamine-Containing Derivative of Cypate (7). We used a similar procedure described for **6** above to prepare **7** from **1** (15 mg, 0.0213 mmol), HBTU (25.8 mg, 0.068 mmol), HOBt (9.2 mg, 0.068 mmol), and a solution of D-(+) glucosamine·HCl (32.4 mg, 0.15 mmol) and DIEA (36.5 mg, 0.28 mmol) in DMSO (1 mL). The crude product was purified by HPLC to afford 6.6 mg (30%) of 7. ES-MS: 947.39 ($[MH]^+$); HR-MS: 947.5096 ($[MH]^+$).

Tri-D-(+)-glucosamine-Containing Derivative of Cypate (8). We used a similar procedure described for **6** above to prepare **8** from **2** (15 mg, 0.0183 mmol), HBTU (38.0 mg, 0.10 mmol) and HOBt (13.5 mg, 0.10 mmol), and a solution of D-(+) glucosamine·HCl (43.2 mg, 0.20 mmol) and DIEA (52.0 mg, 0.40 mmol) in DMSO (1.5 mL). Purification by HPLC afforded 6.0 mg (25%) of **8.** ES-MS: 1223.46 ($[MH]^+$); HR-MS: 1223.4759 ($[MH]^+$).

Tetra-D-(+)-glucosamine-Containing Derivative of Cypate (9). We used a similar procedure described for **6** above to prepare **9** from **3** (16 mg, 0.0171 mmol), HBTU (129.2 mg, 0.34 mmol), HOBt (46.0 mg, 0.34 mmol), and a solution of D-(+) glucosamine·HCl (73.5 mg, 0.34 mmol) and DIEA (129.0 mg, 1.0 mmol) in DMSO (1.5 mL). The mixture was purified by HPLC to afford 7.0 mg (26%) of **9**. ES-MS: 1499.41 ($[MH]^+$).

Hexa-D-(+)-glucosamine-Containing Derivative of Cypate (10). We used a similar procedure described for **6** above to prepare **10** from **4** (20 mg, 0.0172 mmol), HBTU (380.0 mg, 1.0 mmol), HOBt (135 mg, 1.0 mmol), and a mixture of D-(+) glucosamine·HCl (216.0 mg, 1.0 mmol) and DIEA (322.5 mg, 2.5 mmol) in DMSO (8 mL). The crude product was purified by HPLC to afford 7.3 mg (20%) of **10**. ES-MS: 2052.39 ($[MH]^+$), 1026.83 $[MH_2]^{2+}$; HR-MS: 2052.5934 ($[MH]^+$).

Octa-D-(+)-glucosamine-Containing Derivative of Cypate (11). We used a similar procedure described for **6** above to prepare **11** from **5** (20 mg, 0.0143 mmol), HBTU (380 mg, 1.0 mmol), HOBt (135 mg, 1.0 mmol), and a mixture of D-(+) glucosamine·HCl (432.0 mg, 2.0 mmol) and DIEA (516 mg, 4.0 mmol) in DMSO (12.0 mL). HPLC purification afforded 8.0 mg (21%) of **11**. ES-MS: 2606.49 ($[MH]^+$), 1302.47 ($[MH_2]^{2+}$); HR-MS: 2604.5407 ($[MH]^+$).

Solution Stability Studies. The stability of representative probes in four different media was monitored by UV−vis. The test solutions (10 μM) were prepared by adding stock solutions (1 mM, 30 μL) into 2970 μL of five different mediums: aqueous NaOH (0.01 M), aqueous HCl (0.01 M), PBS buffer (pH 7.2), 50% aqueous acetonitrile, and 50% aqueous acetonitrile containing 0.01 M DIEA. The solutions were kept at room temperature or incubated at 37 °C for analysis by UV−vis. The difference between the initial and subsequent absorbances of the solution at λ_{max} for each compound was used to determine their stability under different conditions.

Photostability Studies. Photostability studies were monitored by UV−vis at a probe concentration of 5.56 μM in 20% aqueous DMSO under three different conditions: in the dark (cuvette containing the solution was wrapped in aluminum foil), normal room fluorescent light (monitored at 24 h intervals for one week), and direct exposure to 60 W light bulb (sample was placed 30 cm from the light source and monitored at 0.5 h intervals for 8 h). Changes in the initial and subsequent absorbances of **1**, **5**, and **11** were recorded at the λ_{max} for each compound.

Biodistribution Assays. All animal studies were performed in compliance with the Guidelines for the Care and Use of Research Animals established by Washington University's Animal Studies Committee. To establish tumors, 1×10^7 CA20948 cells, grown in DMEM medium containing 10% fetal calf serum, were injected subcutaneously into the left flank of male nude mice. The CA20948 tumor typically grows to 3−5 mm between 14 and 21 days postinjection. The tumor bearing mice were anesthetized with ketamine/xylazine via intraperitoneal injection and each probe in 20% aqueous DMSO (0.3 μmol/kg body weight) was administered retroorbitally into the mice. At 24 h postinjection, the animals were euthanized and selected organs were removed, washed, and placed on a dark background for fluorescence imaging.

A noninvasive in vivo continuous wave fluorescence imaging apparatus was used to assess the localization and distribution of the probes, as described previously (*12*). Briefly, two 780 nm laser diodes were launched into fiber optic bundles to excite the probes and the emitted fluorescence was captured with a Photometrics CoolSnap HQ charge-coupled device (CCD) camera equipped with an 830 nm interference filter. We used two laser diodes to produce as much uniform illumination of the organs as possible. Images were acquired and processed using WinView software from Princeton Instruments. Tissue parts, instead of whole organs, were used to determine the relative fluorescence intensity in each organ to minimize problems associated with depth-dependent nonlinear fluorescence emission. A statistical program in the WinView package was used to estimate the mean fluorescence intensity per organ part.

RESULTS AND DISCUSSION

Synthesis. *Improved Synthesis of Cypate, the First Generation Dye.* The improved procedure is summarized

Scheme 1. Improved Synthesis of Cypate via Preacylation Approach[a]

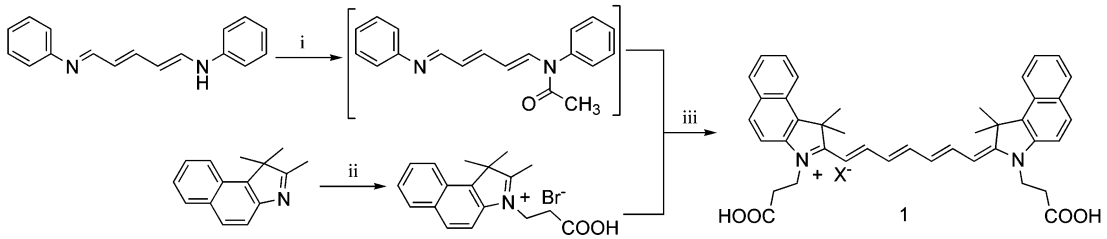

[a] Reagents and conditions: (i) acetic anhydride/DIEA/DCM; (ii) 3-bromopropanoic acid/1,2-dichlorobenzene/110 °C; (iii) CH_3COONa/CH_3CN/H_2O/refluxed.

in Scheme 1. Cypate (**1**) was originally designed to mimic the absorption, fluorescence emission, excretion pathway, and blood clearance profiles of indocyanine green (ICG) because of the in vivo biocompatibility in humans and desirable spectral properties of ICG (*1*, *9*, *11*, *12*). Unlike ICG, **1** can serve as an optical scaffold for multivalent molecular designs because it contains two carboxylic acid functional sites for further derivatization. Initially, we synthesized **1** by a conventional method where a mixture of carboxypropyl benzoindole, glutaconaldehyde dianil monohydrochloride, and sodium acetate were refluxed in ethanol (*12*). Unfortunately, the isolated yield was low (<10%). Consequently, we explored alternative approaches to improve cypate synthesis by optimizing the reaction conditions (*6*, *12*, *16*).

Previous studies indicate that N-acetylation of the intermediate glutaconaldehyde may play an important role in the reaction of aldehydes with benzoindole to form tricarbocyanine dyes (*17*, *18*). This reaction is routinely performed in situ by using a mixture of acetic anhydride/acetic acid. However, the synthesis we conducted in acetic anhydride/acetic acid solution did not improve the yield of **1**. Therefore, we explored preacetylation of glutaconaldehyde with acetic anhydride prior to condensation with benzoindole intermediate at 110 °C to minimize the formation of byproducts generated at higher temperatures. As summarized in Scheme 1, the reaction of 1,1,2-trimethyl-[1H]-benz[*e*]indole and 3-bromopropanoic acid at 110 °C in dichlorobenzene afforded 1,1,2-trimethyl-[1H]-benz[*e*]indole-3-propanoic acid, which was conveniently purified by trituration in DCM and filtration to afford the compound in >80% yield. Reaction of glutaconaldehyde dianil monohydrochloride with acetic anhydride in the presence of triethylamine in DCM afforded acetyl glutaconaldehyde dianil. The solution was added to a refluxing mixture of 1,1,2-trimethyl[1H]-benz[*e*]-indole-3-propanoic acid and sodium acetate in ethanol at 70 °C. The resulting mixture was refluxed for about 16 h, concentrated, and washed with a solution of dilute HCl to afford the desired compound. Although this procedure improved the isolated yield of **1** over previous methods, the purification was still difficult because of the formation of solvent-mediated mono- and diethyl ester byproducts.

After conducting the reactions in different solvent systems, we found that a mixture of acetonitrile/water (7:3) eliminates the ester byproduct formation and significantly increased the isolated yield of **1**. The condensation reaction progressed smoothly at 70 °C in the aqueous acetonitrile solution, suggesting that the dye formation is favored by entropy and higher reaction temperatures are avoidable. The desired compound **1** was obtained in >80% yield by recrystallization. ES-MS, NMR, and HPLC analyses confirmed its identity and purity. The facile workup, non-HPLC-based purification, and gram-scale preparation attest to the importance of preacetylating glutaconaldehyde in reducing the formation of byproducts, making this protocol attractive for efficient large-scale synthesis of **1** and related compounds.

Synthesis of Multivalent Cypate Analogues. The synthetic procedure is summarized in Scheme 2 (*16*). Amide bonds are commonly used as a linker because of its facile formation, derivation to anchor different functionalities, high solution stability, and biocompatibility. For these reasons, we introduced multivalency on carbocyanine dye inner cores via multicarboxamide functionalities. Although the amide formation appears straightforward, we found the use of highly reactive coupling reagents such as HBTU, PyBOP, and HATU in the presence of organic bases such as DIEA lead to the decomposition of **1**, as identified by HPLC, UV−vis, and ES-MS. After evaluating the most commonly used coupling methods, we found that the relatively mild carbodiimide-mediated coupling of **1** and its derivatives with amine-containing compounds gives amide products in good yields. As identified by MS in some reaction mixtures, inactive *N*-acylurea byproducts were formed through O−N migration of the active *O*-acylurea intermediate (*19*). This migration can be minimized by adding HOBt to the reaction mixture, which also catalyzes the reaction. Therefore, we finally used a combination of EDIC/HOBt to prepare the multivalent compounds. Reaction of **1** with di-*tert*-butyl imino diacetate in the presence of EDCI/HOBt, followed by TFA-mediated deprotection, gave two of the second-generation multivalent probes (tri- (**2**) and tetra (**3**) carboxylate-containing derivatives). Further reactions of **2** and **3** with di-*tert*-butyl imino diacetate in the presence of EDIC/HOBt and subsequent TFA-mediated deprotection afforded two of the third-generation multivalent probes (hexa- (**4**) and octa- (**5**) carboxylate-containing derivatives (Scheme 2)). The compounds were purified and obtained in moderate to good yields as follows: **2** (33%), **3** (60%), **4** (30%), and **5** (30%). The NIR multivalent molecular probes were used to prepare dendritic arrays of diverse bioactive moieties on a carbocyanine inner core for molecular recognitions.

Dendritic Arrays of Glucosamine on Carbocyanine Core. Carbohydrates play important roles in molecular recognitions. These polyhydroxylated molecules typically enhance the intended biological event via multivalent interactions in glycoside clusters (*20*). To explore the potentials of the multivalent carbocyanines in molecular recognition studies, we constructed a library of multivalent glucosamine-containing carbocyanine conjugates as molecular beacons. Accordingly, a series of compounds including **6**, **7**, **8**, **9**, **10**, and **11** (Figure 1) were prepared by conjugating D-(+)-glucosamine with **1**, **2**, **3**, **4**, and **5** in the presence of HBTU/HOBT/DIEA in moderate yields (*16*).

HPLC Analysis. The purity and homogeneity of all the glucosamine conjugates were analyzed by HPLC. Figure 2 shows two RP-HPLC chromatograms of compound **5** and its conjugate **11**. Expectedly, conjugation of

Scheme 2. Synthesis of Multi-carboxylic Acid-containing Carbocyanine Dyes[a]

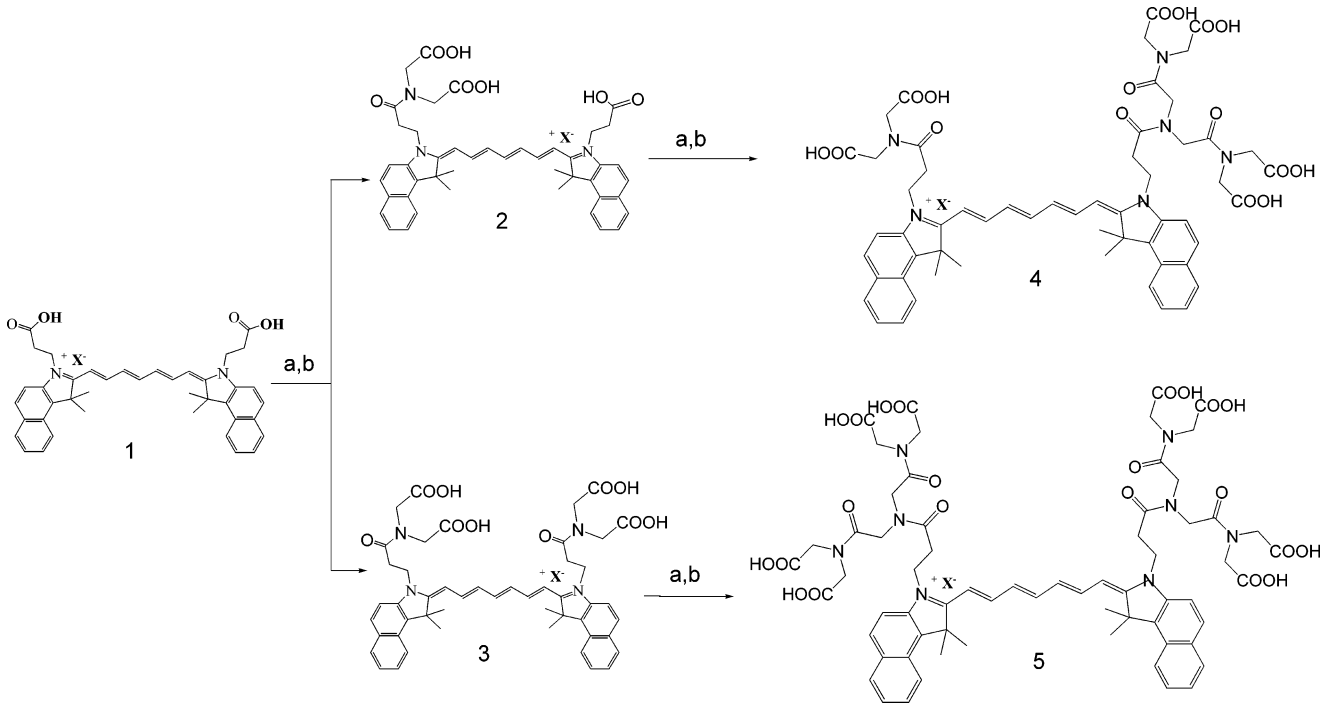

[a]Reagents and conditions: (a) EDCI/HOBT/di-*tert*-butyl iminodiacetate/rt/8 h; (b) TFA.

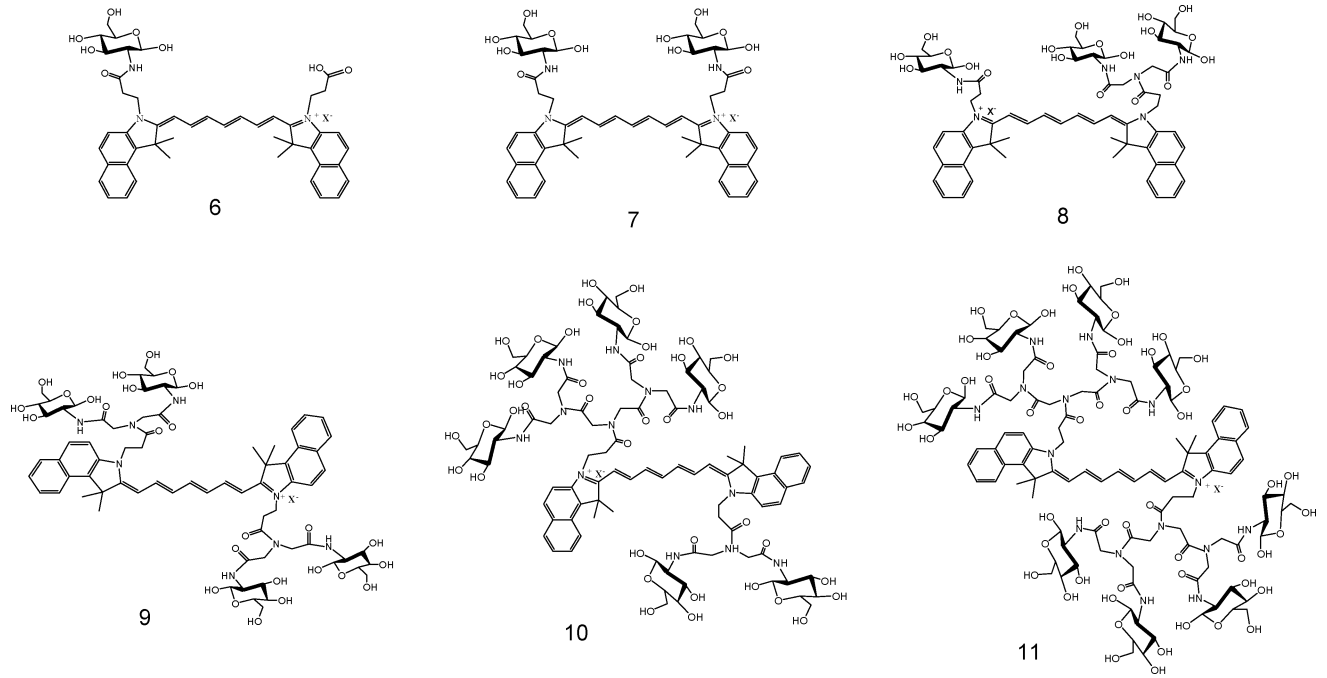

Figure 1. Structures of representative dendritic arrays of glucosamine on an inner NIR carbocyanine core.

the multivalent probes with glucosamine increases the hydrophilicity of the conjugate, as reflected in the shorter HPLC retention time compared with the precursor dye. The enhanced water solubility facilitates formulation of the probes in aqueous buffers for in vivo application.

NMR Analysis. ^{1}H and ^{13}C NMR analysis was performed on representative molecular probes **1**, **5**, and **11**. Structure of **1** was confirmed by proton 1D spectrum and 2D COSY and HMQC experiments. In Figure 3(A), the doublet at 6.45 ppm is assigned to the terminal protons at the conjugated double bond that are next to the indole ring. Spin propagation from the center proton (a in Figure 4(A)) toward the terminal proton (d in Figure 4A) further confirms the symmetrically conjugated seven-carbon double-bonded fragment. Assigned carbon resonances range from 104 to 156 ppm in HMQC (Figure 4B, a, b, c, d), indicating the conjugated double bonds are indeed present in **1**. Compounds **5** and **11** were identified by comparing their ^{13}C spectra with **1**. Additional resonances at 168−171 ppm and 47−50 ppm (Figure 5B) confirm the presence of octacarboxylic acid and 12 methylene groups, respectively, in **5**. Furthermore, the spectrum in Figure 5C indicates that the sugar carbons in **11** spans from 54 to 95 ppm. Comparison of the 2D HMQC spectra between **5** and **11** confirms the presence of glucosamine's anomeric H1′ protons at 4.92 and 4.43 ppm while those of H2′ to H6′ range from 3.02 to 3.59 ppm (Figure 6). Proton integration suggests that there is a 6:2 ratio between the

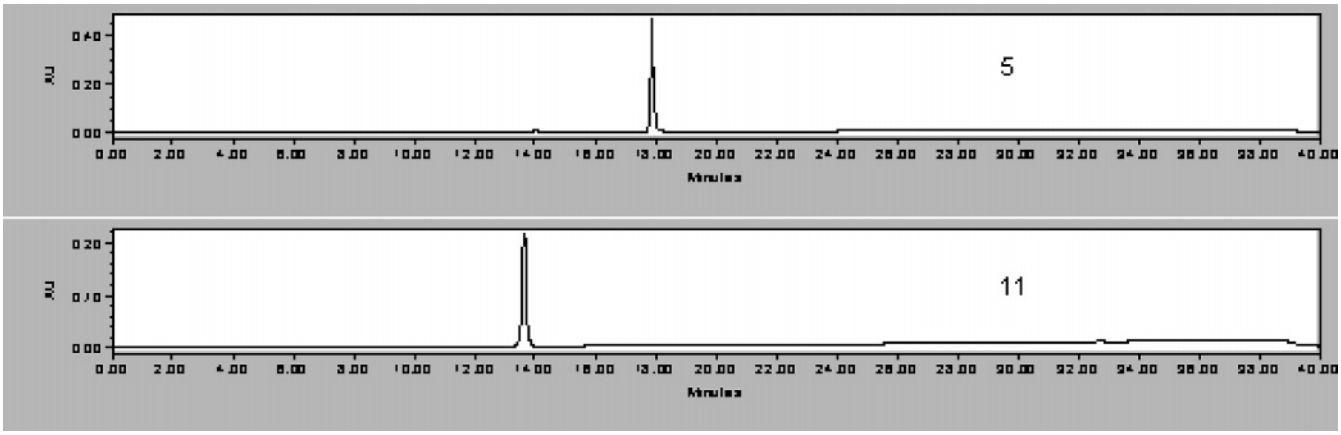

Figure 2. HPLC profiles of compound **5** (top) and **8** (bottom) detected at 254 nm.

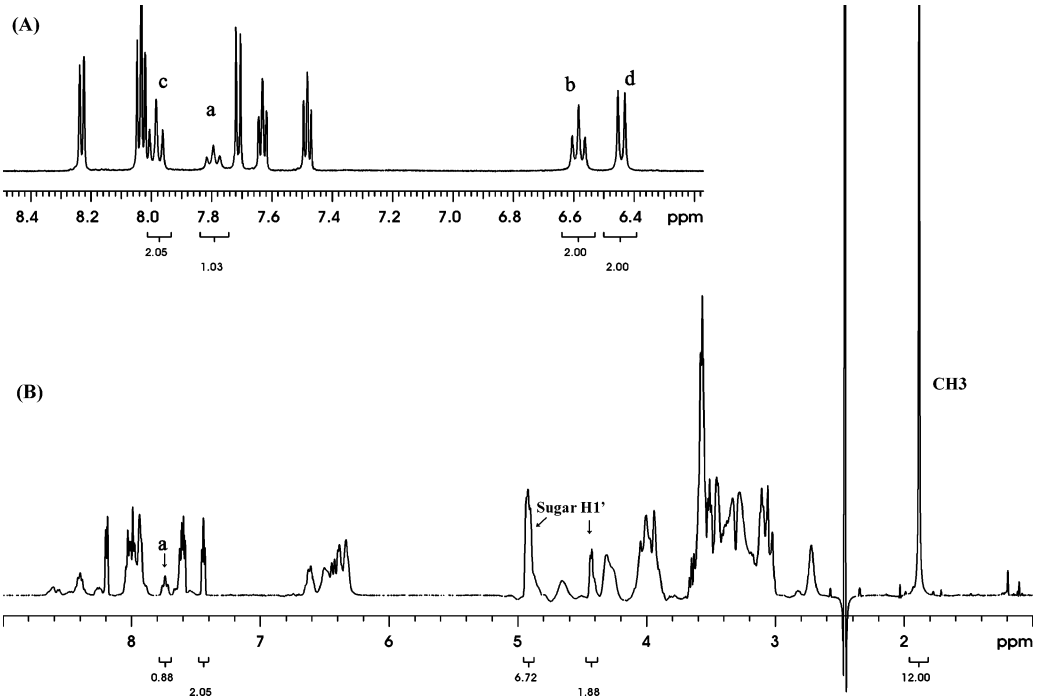

Figure 3. 600 MHz proton spectra of (A) compound **1**, and (B) compound **11** in DMSO-d_6 at 25 °C. Resonance a: center proton, d: terminal vinyl protons next to indole ring, b: protons adjacent to a, and c: protons adjacent to d.

two H1′ resonances (Figure 3B) and further confirms **11** possesses eight sugar moieties in the structure.

Absorption and Emission Properties. The absorption and emission spectra of all the compounds evaluated are similar, with their maxima centered around 780 and 810 nm, respectively. Figure 7 shows the normalized absorption and emission spectra of **1**, **5**, and **11**. Expectedly, the spectral properties of the dendritic arrays are also similar to the precursor multivalent beacons in the same solvent because conjugation occurred at distal positions to the inner chromophore core. This feature demonstrates another advantage of this series of multivalent molecular probes in providing consistent and predictable spectral properties for biological applications. All the compounds have exceptionally high molar absorptivity in a variety of solvents (Table 1).

Solution Stability Studies. Understanding the stability of molecular probes in different solvent systems will guide researchers in selecting the appropriate medium to formulate the compounds, perform reactions, and optimize storage conditions for each probe. To this effect, we assessed the stabilities of **1** (precursor dye), **5** (carboxylic acid tethered multivalent dye), and **11** (dendritic array of glucosamine on the multivalent dye **5**) in different mediums and temperatures. Dilute NaOH and HCl were chosen to represent the mild basic or acidic conditions frequently encountered in diverse applications. Because we typically lyophilize the compounds in aqueous acetonitrile (ACN) and conduct reactions in DIEA-containing organic solutions, we also evaluated the stabilities of the probes in 50% aqueous ACN and 0.01 M DIEA solution in 50% aqueous ACN. Phosphate-buffered saline (PBS, pH 7.2) is conventionally used to formulate products for biological applications, and hence prolonged stability of the probes in PBS is highly desirable. The stabilities of the probes (10 μM) in different mediums were monitored by UV−vis at λ_{max} of each probe.

As with most carbocyanine dyes, all the compounds tested are relatively stable in acidic condition at room temperature (Figure 8) and 37 °C (Figure 9). Possibly, protonation of the "donor" tertiary amine of the benzoindole carbocyanine stabilizes the probes. Similarly, solutions of the probes in 50% aqueous ACN are exceptionally stable for up to 18 h at 37 °C. These results suggest that workup and storage conditions in acidic and aqueous

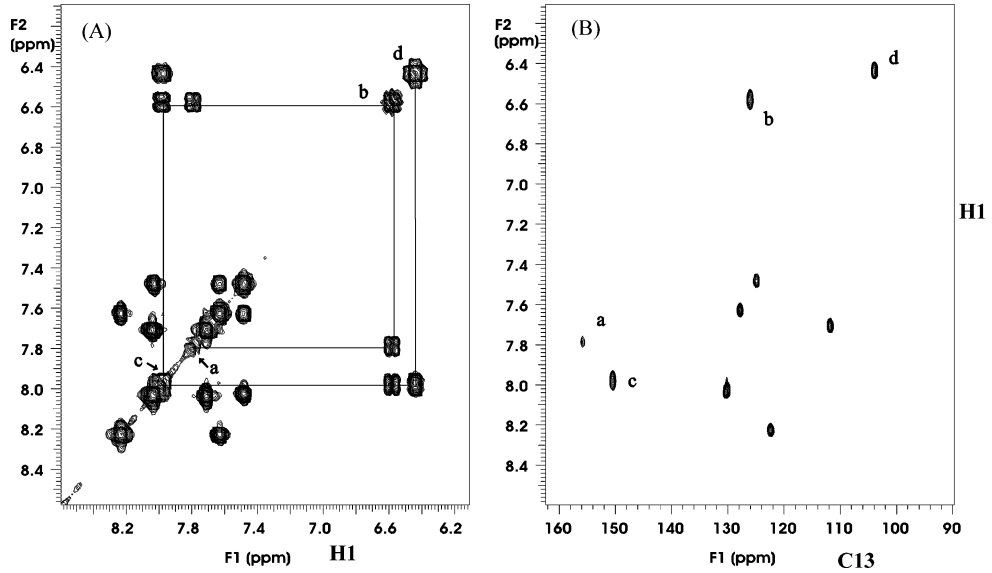

Figure 4. Expansions of the 600 MHz (A) COSY and (B) HMQC spectra of compound **1** in DMSO-d_6 at 25 °C. Same figure labels as in Figure 1.

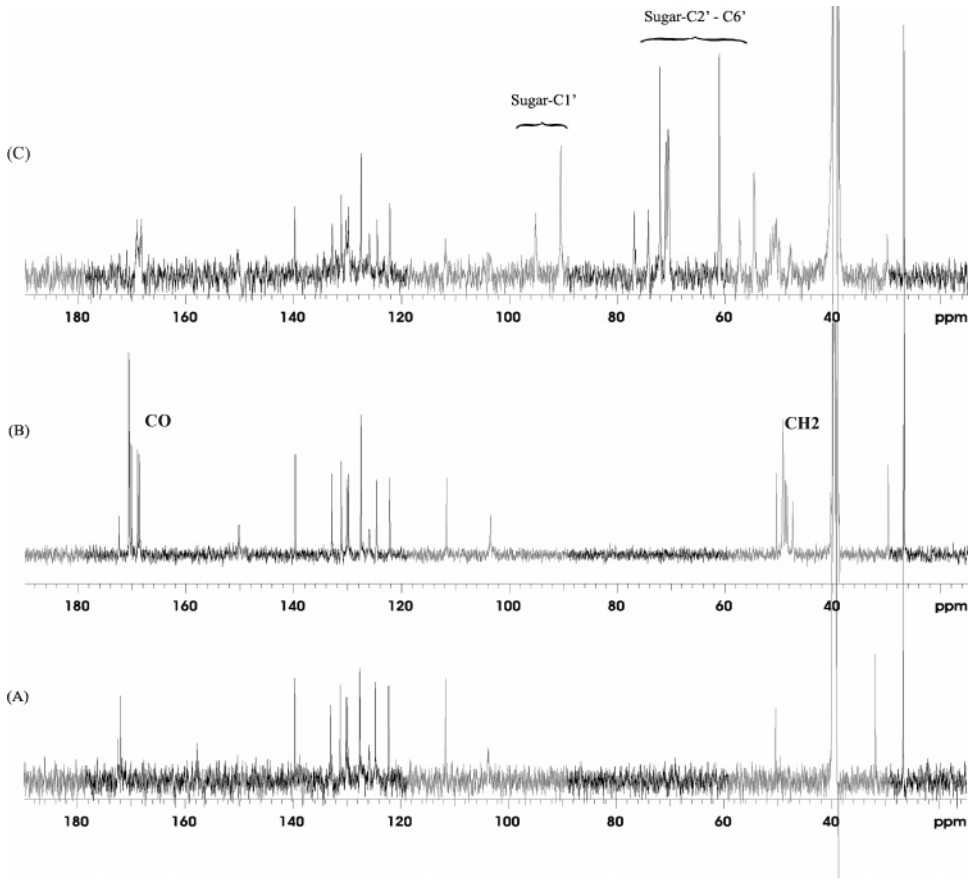

Figure 5. Carbon-13 spectra of (A) compound **1**, (B) compound **5**, and (C) compound **11** in DMSO-d_6 at 25 °C.

ACN mediums do not destabilize the chromophore system. In contrast, stabilities of the compounds in NaOH were different. While **5** was relatively stable in this medium up to 96 h, **1** and **11** were adversely affected. At 16 h, the percent absorbance of **1** in NaOH decreased to <80% and further dropped to <30% at room temperature after 96 h (Figure 8). A similar trend was obtained at 37 °C (Figure 9). This mild but progressive destabilization of **1** in NaOH may be due to the initial formation of the sodium carboxylate salt, followed by the generation of hydroxide zwitterions with the quartenary amine group of benzoindole. The strong basic hydroxide counterion can destabilize the conjugated π-system by abstracting acidic protons or reversing the aldehyde−trimethylbenzoindole condensation (Scheme 1). This inner salt effect by a strong basic counterion is supported by the minimal destabilization of **1** in the mild basic DIEA solution in aqueous ACN (Figure 9). Stability of **11** in basic mediums is abysmal and appears to correlate with the basicity of the medium, with stability in NaOH < DIEA solutions. This can be attributed to the hydrolysis of the glucosamine moieties under basic conditions, which gener-

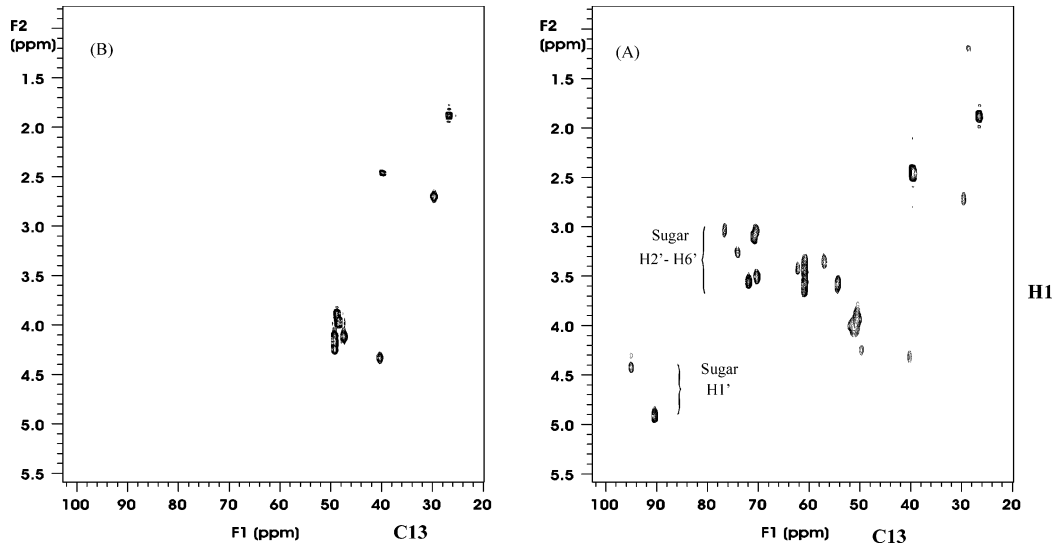

Figure 6. Expansions of the 600 MHz HMQC spectra of (a) compound **11** and (b) compound **5** in DMSO-d_6 at 25 °C.

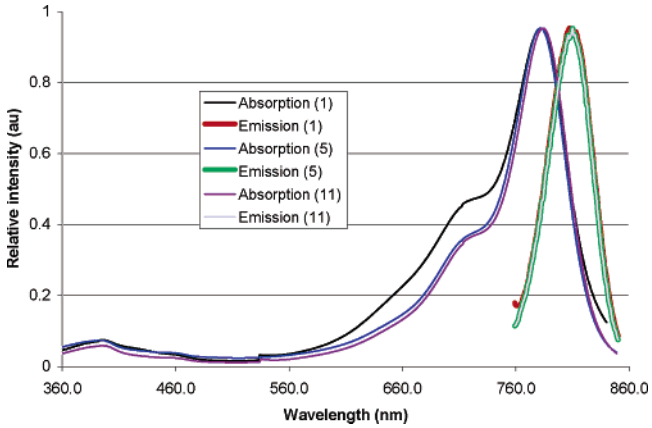

Figure 7. Normalized absorption and emission spectra of **1**, **5**, and **11** in 20% aqueous DMSO.

ates a mixture of byproducts that interfere with the spectral properties of the probe. Based on HPLC profile (not shown), the retention time of the byproducts (10.9 min), which increased in intensity as a function of time, is close to that of **5** (11.7 min) under the same HPLC condition, suggesting an incomplete hydrolysis of **11** toward the precursor probe **5**. However, **11** is most stable in PBS relative to **1** and **5** at room temperature after 96 h (Figure 8). This interesting observation indicates that the dendritic glucosamine probes can be formulated and stored in PBS for biological assays.

The results of the solution stability studies show that constructing multivalency on an inner chromophore core produced a robust NIR multivalent molecular probe (**5**) with exceptionally high stability in different mediums and at physiologically relevant temperatures, compared with the precursor dye (**1**). Stability of the dendritic array of biomolecules on the multivalent probes depends on the inherent stability of the biomolecule itself. In this study, the glucosamine cluster (**11**) is remarkably stable in acidic (dilute aqueous HCl) and buffered (PBS, pH 7.2) solutions but unstable under basic conditions.

Photostability Studies. Photostability studies were performed at a concentration of 5.56 μM in 20% aqueous

Table 1. Photophysical Properties of NIR Multivalent Probes in Different Solvents

compd	solvent	λ_{max}^{ab} (nm)	λ_{max}^{em} (nm)	$\Delta\lambda$ (nm)	ϵ (10^5) mol^{-1} cm^{-1}	compd	solvent	λ_{max}^{ab} (nm)	λ_{max}^{em} (nm)	Δ_λ (nm)	ϵ (10^5) mol^{-1} cm^{-1}
1	20% DMSO	782	808	26	2.24	**7**	20% DMSO	783	810	27	2.24
	PBS (pH 7.2)	778	805	27			PBS (pH 7.2)	779	805	26	
	water	778	803	25			water	779	806	27	
	95% ethanol	787	816	29			95% ethanol	786	813	27	
2	20% DMSO	782	812	30	1.90	**8**	20% DMSO	784	811	27	1.97
	PBS (pH 7.2)	778	806	28			PBS (pH 7.2)	780	806	26	
	water	778	805	27			water	779	806	27	
	95% ethanol	785	814	29			95% ethanol	789	814	25	
3	20% DMSO	782	808	26	2.15	**9**	20% DMSO	783	808	25	1.87
	PBS (pH 7.2)	777	807	30			PBS (pH 7.2)	779	809	30	
	water	777	805	28			water	779	809	30	
	95% ethanol	785	813	28			95% ethanol	783	812	29	
4	20% DMSO	782	808	26	2.01	**10**	20% DMSO	784	809	25	2.19
	PBS (pH 7.2)	778	805	27			PBS (pH 7.2)	780	808	28	
	water	778	811	33			water	780	808	28	
	95% ethanol	785	814	29			95% ethanol	792	819	27	
5	20% DMSO	782	810	28	1.85	**11**	20% DMSO	784	810	26	1.99
	PBS (pH 7.2)	778	804	26			PBS (pH 7.2)	780	807	27	
	water	778	810	32			water	780	807	27	
	95% ethanol	787	814	27			95% ethanol	791	816	25	
6	20% DMSO	783	809	26	2.24						
	PBS (pH 7.2)	778	805	27							
	water	778	806	28							
	95% ethanol	786	815	29							

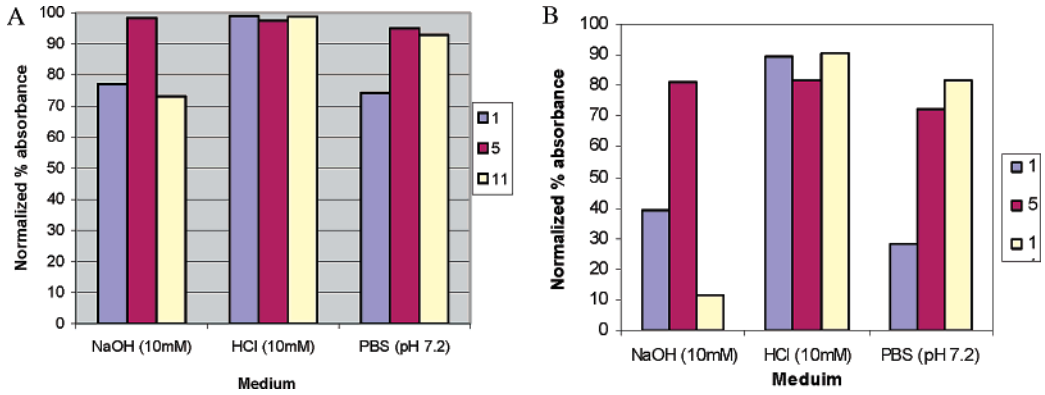

Figure 8. Absorbance of **1**, **5**, and **11** in different mediums at room temperature: (A) 16 h and (B) 96 h. The initial absorbance at $t = 0$ for each medium is normalized as 100%.

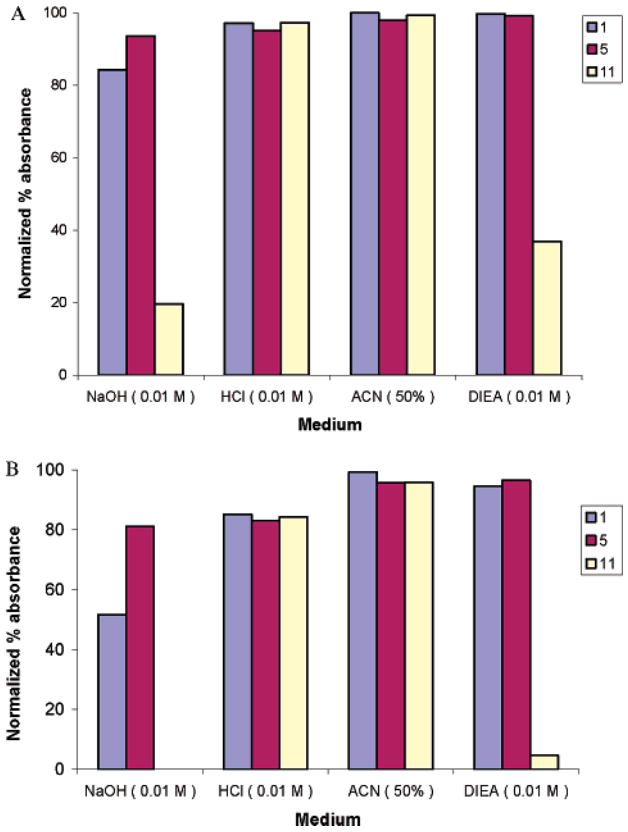

Figure 9. Absorbance of **1**, **5**, and **11** in different mediums at room temperature: (A) 16 h and (B) 96 h. The initial absorbance at $t = 0$ for each medium is normalized as 100%.

DMSO under three different conditions. A solution of the probe in a cuvette was (1) wrapped in aluminum foil and stored in a dark room, (2) placed on a laboratory shelf and exposed to normal fluorescent room light (condition A), and (3) exposed to a bright 60 W light bulb placed within 30 cm from the sample (condition B). UV−vis spectra were recorded at 0.5 h intervals for over 8 h under condition B and at 24 h intervals over one week for condition A. We found that the photophysical stability of all the molecular probes were identical. In the dark, the absorbance remained nearly constant for >1 week. Under fluorescent room light, no appreciable change in absorbance was observed for up to 24 h. However, the absorbance gradually decreased to 20% after 5 days. In contrast, all of the solutions were very unstable on exposure to bright light (Figure 10). The decrease in absorbance appears to follow a two-phase exponential model with a linear decay constant of about $-7.2\ s^{-1}$. The photostability data demonstrates that the multivalency does not protect the chromophore system from photodegradation and that the conventional storage in the dark is still recommended for the multivalent compounds. The observed decrease is probably due to photobleaching.

In Vivo Biodistribution. Glucose is the primary monosaccharide from carbohydrate digestion that is transported to cells to generate energy for normal physiological functions. Internalization of glucose in cells is typically mediated by glucose transporters (GLUTs) where it is phosphorylated by mitochondrial hexokinase (*21*). The metabolic fate of glucose hinges on the intricate interplay between extracellular glucose level, GLUTs and mitochondrial hexokinase. Abnormal, hypermetabolizing cells such as cancers, overexpress GLUTs to enhance this equilibrium-dependent glucose transport relative to normal surrounding cells. Therefore, molecules that are recognized by GLUTs but not further metabolized once internalized in cells accumulate in diseased tissues, thereby providing a method to image and treat pathologic tissues. This strategy is widely used to image hypermetabolizing cells by positron emission tomography after administering a radioactive glucose analogue, ^{18}fluorodeoxyglucose (^{18}FDG) to patients (*22*). Previous studies have shown that a fluorescent probe-labeled glucosamine derivative, 2-(*N*-(7-nitrobenz-2-oxa-1,3- diazol-4-yl)amino)-2-deoxyglucose (2-NBDG), is a viable nonradioactive method to monitor glucose transport and uptake in cells (*23*). More recent studies have shown that conjugation of glucosamine to NIR fluorescent dyes (*24*) or photosensitizers (*25*) results in high tumor uptake of the compounds. Although carbohydrates are known to interact strongly with their target via glycosidic clusters (*20*), these studies did not explore the potential beneficial effects of multivalency. Therefore, we evaluated the in vivo distribution of the NIR fluorescent dendritic arrays of glucosamine in highly proliferating pancreatic tumor (CA20948) bearing mice.

Each mouse received 0.3 μmol of the beacons per kg body weight of mouse via tail vein injection. The in vivo and ex vivo distribution of the molecular beacons were monitored by NIR fluorescence imaging using two collimated solid 780 nm laser sources for excitation and a CCD camera equipped with 830 nm interference filter to capture the fluorescence emission (*12*). At 24 h postinjection, the nude mice were sacrificed. Aliquots of blood and some major organs were harvested and washed with distilled water. The mean fluorescence count in each tissue was determined for each compound and normalized relative to 100% of the organ with highest fluorescence intensity (Figure 11). Negative control studies show that the precursor dye **1** was not retained in the tumor

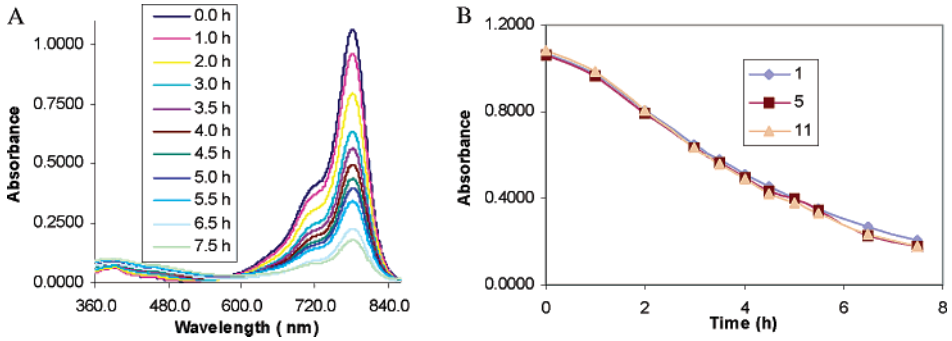

Figure 10. Spectra of the changes in the absorbance of **5** with time and (B) photostability of **1**, **5**, and **11** in 20% aqueous DMSO exposed to 60 W light bulb.

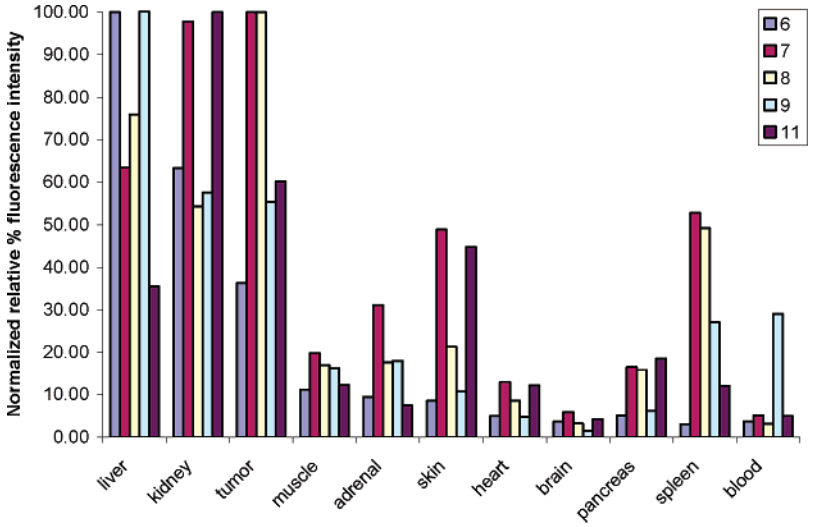

Figure 11. Biodistribution of dendritic arrays of glucosamine in CA20948 pancreatic tumor-bearing mice at 24 h postinjection of the probes.

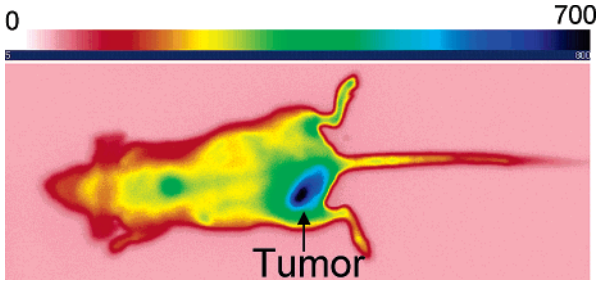

Figure 12. False color fluorescence image of compound **8** in CA20948 tumor-bearing nude mouse at 24 h postinjection of the probe.

but accumulated in the liver at about 1 h postinjection. This observation was also noted in previous studies with the same tumor model in male Lewis rats (*9*, *12*).

In contrast, all of the dendritic arrays of glucosamine were retained in the tumor up to 24 h postinjection (Figure 11). Compounds **7** and **8** have the highest tumor uptake at 24 h postinjection. However, the high retention of **7** in the skin increases background fluorescence, which is not desirable for noninvasive optical imaging. A significant amount of compound **9** is retained in blood at 24 h postinjection, making it the best agent for applications that require long-circulating probes with low skin uptake. The octaglucosamine probe (**11**) rapidly accumulates in the target tumor tissue within 6 h postinjection but at 24 h, the tumor uptake reduced to about 50% of the fluorescence intensity relative to the kidneys, which became the predominant retention organ. Surprisingly, the skin uptake of **11** was also high. Of all the glucosamine derivatives examined, the triglucosamine derivative (**8**) appears to have a good balance between high tumor uptake and decreased retention in nontarget tissues (Figure 12). Overall, there is an intricate relationship between the probe distribution and the multivalent compounds but the molecular basis for the selective uptake in some tissues is not clear at this time. Nonetheless, these results demonstrate that each compound can be used for different biomedical applications. For example, compound **9**, which is retained in blood for >24 h, could serve as a blood pool agent for monitoring blood flow and imaging blood vessels.

CONCLUSION

NIR carbocyanine dyes can effectively serve as optical scaffold for anchoring multiple functionalities and providing multivalency for molecular recognition studies. On the basis of the synthetic strategy developed, higher generations of the multivalent compounds are also accessible. Because the reactive functional groups are distal to the chromophore core, both multicarboxylate probes and their dendritic glucosamine derivatives have similar spectral properties, thereby improving data reproducibility and enabling the use of the same excitation source and filter for sample analysis. Photophysical stability studies show that neither the multivalent probes nor their corresponding dendritic array of biomolecules confer greater photostability to the chromophore core relative to the precursor dye. However, the multivalency appears to remarkably enhance the solution stability of the multicarboxylate probes in different mediums at physi-

ologically relevant temperatures. Overall, the stability studies provide guidance for reaction mediums and storage conditions. Biodistribution studies in tumor-bearing nude mice showed that all the glucosamine conjugates localized in the tumor but the precursor dye, cypate was almost exclusively retained in the liver. The pattern of probe distribution in various tissues suggests that each of the NIR fluorescent glucosamine derivatives could be useful for different but complimentary biological applications.

ACKNOWLEDGMENT

Funding for this project was provided by the NSF Bioengineering grant (BES 0119489).

LITERATURE CITED

(1) Hawrysz, D. J., and Sevick-Muraca, E. M. (2000) Developments toward diagnostic breast cancer imaging using near-infrared optical measurements and fluorescent contrast agents. *Neoplasia 2*, 388−417.

(2) Mahmood, U., and Weissleder, R. (2003) Near-infrared optical imaging of proteases in cancer. *Mol. Cancer Ther. 2*, 489−496.

(3) Tung, C. H., Mahmood, U., Bredow, S., and Weissleder, R. (2000) In vivo imaging of proteolytic enzyme activity using a novel molecular reporter. *Cancer Res. 60*, 4953−4958.

(4) Achilefu, S. (2004) Lighting up tumors with receptor-specific optical molecular probes. *Technol. Cancer Res. Treat. 3*, 393−409.

(5) Sevick-Muraca, E. M., Houston, J. P., and Gurfinkel, M. (2002) Fluorescence-enhanced, near-infrared diagnostic imaging with contrast agents. *Curr. Opin. Chem. Biol. 6*, 642−650.

(6) Ye, Y., Li, W. P., Anderson, C. J., Kao, J., Nikiforovich, G. V., et al. (2003) Synthesis and characterization of a macrocyclic near-infrared optical scaffold. *J. Am. Chem. Soc. 125*, 7766−7767.

(7) Frangioni, J. V. (2003) In vivo near-infrared fluorescence imaging. *Curr. Opin. Chem. Biol. 7*, 626−634.

(8) Becker, A., Hessenius, C., Licha, K., Ebert, B., Sukowski, U., et al. (2001) Receptor-targeted optical imaging of tumors with near-infrared fluorescent ligands. *Nat. Biotechnol. 19*, 327−331.

(9) Bugaj, J. E., Achilefu, S., Dorshow, R. B., and Rajagopalan, R. (2001) Novel fluorescent contrast agents for optical imaging of in vivo tumors based on a receptor-targeted dye-peptide conjugate platform. *J. Biomed. Opt. 6*, 122−133.

(10) Achilefu, S., Jimenez, H. N., Dorshow, R. B., Bugaj, J. E., Webb, E. G., et al. (2002) Synthesis, in vitro receptor binding, and in vivo evaluation of fluorescein and carbocyanine peptide-based optical contrast agents. *J. Med. Chem. 45*, 2003−2015.

(11) Ntziachristos, V., Yodh, A. G., Schnall, M., and Chance, B. (2000) Concurrent mri and diffuse optical tomography of breast after indocyanine green enhancement. *Proc. Natl. Acad. Sci. U.S.A. 97*, 2767−2772.

(12) Achilefu, S., Dorshow, R. B., Bugaj, J. E., and Rajagopalan, R. (2000) Novel receptor-targeted fluorescent contrast agents for in vivo tumor imaging. *Invest. Radiol. 35*, 479−485.

(13) Mammen, M., Choi, S. K., and Whitesides, G. M. (1998) Polyvalent interactions in biological systems: Implications for design and use of multivalent ligands and inhibitors. *Angew. Chem.-Int. Edit. 37*, 2755−2794.

(14) Yordanov, A. T., Kobayashi, H., English, S. J., Reijnders, K., Milenic, D., et al. (2003) Gadolinium-labeled dendrimers as biometric nanoprobes to detect vascular permeability. *J. Mater. Chem. 13*, 1523−1525.

(15) Gopidas, K. R., Whitesell, J. K., and Fox, M. A. (2003) Nanoparticle-cored dendrimers: Synthesis and characterization. *J. Am. Chem. Soc. 125*, 6491−6502.

(16) Ye, Y. P., Bloch, S., and Achilefu, S. (2004) Polyvalent carbocyanine molecular beacons for molecular recognitions. *J. Am. Chem. Soc. 126*, 7740−7741.

(17) Becker, A., Riefke, B., Ebert, B., Sukowski, U., Rinneberg, H., et al. (2000) Macromolecular contrast agents for optical imaging of tumors: Comparison of indotricarbocyanine-labeled human serum albumin and transferrin. *Photochem. Photobiol. 72*, 234−241.

(18) Lin, Y. H., Weissleder, R., and Tung, C. H. (2002) Novel near-infrared cyanine fluorochromes: Synthesis, properties, and bioconjugation. *Bioconjugate Chem. 13*, 605−610.

(19) Volonterio, A., and Zanda, M. (2003) Domino condensation/aza-michael/o→n acyl migration of carbodiimides with activated [alpha],[beta]-unsaturated carboxylic acids to form hydantoins. *Tetrahedron Lett. 44*, 8549−8551.

(20) Bolam, D. N., Xie, H. F., White, P., Simpson, P. J., Hancock, S. M., et al. (2001) Evidence for synergy between family 2b carbohydrate binding modules in cellulomonas fimi xylanase 11a. *Biochemistry 40*, 2468−2477.

(21) Pauwels, E. K. J., Ribeiro, M. J., Stoot, J., McCready, V. R., Bourguignon, M., et al. (1998) Fdg accumulation and tumor biology. *Nucl. Med. Biol. 25*, 317−322.

(22) Gambhir, S. S. (2002) Molecular imaging of cancer with positron emission tomography. *Nat. Rev. Cancer 2*, 683−693.

(23) Yamada, K., Nakata, M., Horimoto, N., Saito, M., Matsuoka, H., et al. (2000) Measurement of glucose uptake and intracellular calcium concentration in single, living pancreatic beta-cells. *J. Biol. Chem. 275*, 22278−22283.

(24) Chen, Y., Zheng, G., Zhang, Z. H., Blessington, D., Zhang, M., et al. (2003) Metabolism-enhanced tumor localization by fluorescence imaging: In vivo animal studies. *Opt. Lett. 28*, 2070−2072.

(25) Zhang, M., Zhang, Z. H., Blessington, D., Li, H., Busch, T. M., et al. (2003) Pyropheophorbide 2-deoxyglucosamide: A new photosensitizer targeting glucose transporters. *Bioconjugate Chem. 14*, 709−714.

BC049790I